MOLECULAR BIOLOGY & GENETICS

RESEARCH ARTICLE

Transgenic rhesus monkeys carrying the human MCPH1 gene copies show human-like neoteny of brain development

Lei Shi[1,2,3]†, Xin Luo[1,2,3,10]†, Jin Jiang[1,2,3,10]†, Yongchang Chen[4]†, Cirong Liu[7]†, Ting Hu[1,2,3,10], Min Li[1], Qiang Lin[1], Yanjiao Li[1], Jun Huang[1], Hong Wang[4], Yuyu Niu[4], Yundi Shi[5], Martin Styner[5,6], Jianhong Wang[7], Yi Lu[8], Xuejin Sun[8], Hualin Yu[9], Weizhi Ji[4*], Bing Su[1,2,3*]

[1] State Key Laboratory of Genetic Resources and Evolution, Kunming Institute of Zoology, Chinese Academy of Sciences, Kunming 650223, China.

[2] Primate Research Center, Kunming Institute of Zoology, Chinese Academy of Sciences, Kunming 650223, China.

[3] Center for Excellence in Animal Evolution and Genetics, Chinese Academy of Sciences, Kunming 650223, China.

[4]Yunnan Key Laboratory of Primate Biomedical Research, Institute of Primate Translation Medicine, Kunming University of Science and Technology, Kunming, 650500, China.

[5]Department of Psychiatry, University of North Carolina, Chapel Hill, NC 27599-7160, USA

[6]Department of Computer Science, University of North Carolina, Chapel Hill, NC 27599-7160, USA.

[7]Key Laboratory of Animal Models and Human Disease Mechanisms, Kunming Institute of Zoology, Chinese Academy of Sciences, Kunming, 650223, China

[8]Department of Medical Imaging, the First Affiliated Hospital of Kunming Medical University, Kunming, 650032, China

[9]Department of Minimally Invasive Neurosurgery, the First Affiliated Hospital of Kunming Medical University, Kunming, 650032, China

[10]Kunming College of Life Science, University of Chinese Academy of Sciences, Beijing 100101, China.

† Equally contributed to this work.

*Correspondence and requests for materials should be addressed to B.S. (sub@mail.kiz.ac.cn) or W. J. (wji@lpbr.cn).

Abstract

Brain size and cognitive skills are the most dramatically changed traits in humans during evolution, and yet the genetic mechanisms underlying these human-specific changes remain elusive. Here, we successfully generated 11 transgenic rhesus monkeys (8 first-generation and 3 second-generation) carrying human copies of *MCPH1*, an important gene for brain development and brain evolution. Brain image and tissue section analyses indicated an altered pattern of neural cell differentiation, resulting in a delayed neuronal maturation and neural fiber myelination of the transgenic monkeys, similar to the known evolutionary change of developmental delay (neoteny) in humans. Further brain transcriptome and tissue section analyses of major developmental stages showed a marked human-like expression delay of neuron-differentiation and synaptic signaling genes, providing a molecular explanation to the observed brain developmental delay of the transgenic monkeys. More importantly, the transgenic monkeys exhibited better short-term memory and shorter reaction time compared to the wild type controls in the delayed matching to sample task. The presented data represents the first attempt to experimentally interrogate the genetic basis of human brain origin using a transgenic monkey model, and it values the use of nonhuman primates in understanding human unique traits.

Keywords: human evolution, brain development, MCPH1, transgenic monkey, neoteny, cognition

Received: 19-Feb-2019; Revised: 06-Mar-2019; Accepted: 18-Mar-2019.

Introduction

Expansion in brain size and improvement in cognitive skills are among the most fundamental evolutionary changes that set humans apart from other primates. Comparative genomic analyses between humans and nonhuman primates suggest that these dramatic phenotypic divergences may be due to several underlying genetic changes:

rapid evolution of protein coding genes [1, 2] and non-coding RNA genes [3-5], emergence of human-specific segmental duplications [6-8], as well as alterations in gene expression [9-12] and epigenetic regulation [13-15]. Though a lot of efforts in previous studies, we are still on the way of searching for the responsible genes and dissecting the genetic mechanisms that shape up the human brain.

Among the reported genes that play important roles in human brain development, *MCPH1* (also known as *BRIT1*) is one of the strong candidates that may contribute to human brain evolution [16]. It is one of the fast-evolving genes in primates [17]. In particular, *MCPH1* has accumulated seven human-specific amino acid changes that are fixed in modern humans [17]. Our previous *in vitro* experiments showed that these human-specific protein sequence changes could alter the regulation of *MCPH1* on its downstream genes [18]. Importantly, at transcriptional level, *MCPH1* also showed human-specific changes. During postnatal brain development, *MCPH1* is abundantly expressed in humans, but less in non-human primates (macaque and chimpanzee, Fig.S1A) [11]. In addition, we have shown that the *MCPH1* transcriptional activity was significantly higher in human than in rhesus monkey [18]. Collectively, current evidences suggest that not only the human-specific protein sequence changes, but also gene expression alteration of *MCPH1* may contribute to human brain development and function.

MCPH1 encodes a pleiotrophic protein. It functions as a transcription factor by interacting with E2F1 (E2F transcription factor 1) to regulate cell cycle and cell apoptosis [19]. It also works as a DNA damage response protein, and is inovled in chromatic remodeling to control DNA repair [16, 20, 21]. In the central nervous system, as a centrosome protein, MCPH1 plays a conserved role in neurogenesis by regulating neuronal progenitor divison mode via the Chk1-Cdc25B pathway [22]. In humans, truncated mutations of *MCPH1* cause primary microcephaly (MCPH, OMIM251200), a rare human brain developmental disorder, characterized by significantly reduced brain volume and mental retardation [23-25]. Consistently, the *MCPH1* knockout animal models (mouse and monkey) reproduced the phenotypes of human microcephaly, notably the reduced brain size [22, 26]. During human brain development, *MCPH1* has the highest expression at prenatal stage and the expression reduces after birth and remain a

constant level through adulthood (Fig.S1B). At prenatal stage, *MCPH1* is highly expressed in all cell types in the cortex, including neural progenitor cells, interneurons, astrocytes and microglia cells [27] (Fig. S1B). In mouse study, it was demonstrated that *MCPH1* controls precise mitotic spindle orientation and regulates the progenitor division mode to maintain brain size [22]. However, although *MCPH1* loss of function causes abnormal brain development, resulting in a reduced brain size in human and animals, the functional consequence of the human-specific seqence and expresion changes remains to be understood.

To interrogate the genetic basis of human brain evolution, the traditional mouse or rat models are less ideal due to the vast dissimilarities in brain size and structure between humans and rodents. Instead, a nonhuman primate transgenic model would be far more effective. The rhesus monkey (*Macaca mulatta*), an Old World Monkey species widely used for biomedical research, is an ideal choice, due to its high sequence similarity with humans (>93% for protein coding genes) [28] and yet relatively large phylogenetic distance (about 25 million years of divergence from humans), which alleviates ethical concerns [29].

For *MCPH1*, the coding sequence similarity is 94.9% between human and rhesus monkey, while it is only 67.5% between human and mouse. Similarly, the 5' non-coding sequence (~5kb) of *MCPH1* likely contains regulatory elements for gene expression regulation, and it has 88.7% similarity between human and rhesus monkey, while it is only 40.4% between human and mouse. Additionally, we have shown that during primate evolution, the *MCPH1* promoter region has acquired a primate specific E2F1 binding motif, which is absent in rodents and other mammalian species [30]. Taken together, a rhesus monkey model is promising to study the functional impact of the human-specific changes (protein sequence and gene expression) on human brain evolution.

In this study, to mimic the human-specific genetic changes, using lentivirus transfection, we introduced the human *MCPH1* copies (huMCPH1) into the rhesus monkey genome so that the transgenic (TG) monkeys have an overexpression of human *MCPH1*. We successfully generated 8 first-generation (F1) and 3 second generation (F2) TG monkeys carrying human *MCPH1* copies. Brain development tracking *via* MRI, tissue section with cellular markers showed that the TG monkeys experienced delayed

neuronal maturation and neural fiber myelination, both of which are human-like features of brain-developmental neoteny. Accordingly, transcriptome analysis of prenatal and postnatal brain development revealed an altered gene expression profile in neuro-progenitors and neurons with shifted expression time of synapse related genes in the TG monkeys. Remarkably, our preliminary cognitive test detected an improved short-term memory in the TG monkeys.

Results

Generation of transgenic monkeys carrying human MCPH1 copies

Lentivirus delivery was used to introduce the human *MCPH1* copy (huMCPH1) into the rhesus monkey genome. A high titer (>$1x10^{10}$ infection particles per ml) SIV-vector containing lentivirus was produced for gene transfer (Fig.S1C; see methods for more details). The human *MCPH1* gene was cloned into the SIV vector containing an eGFP (enhanced green fluorescent protein) gene copy and a universal promoter (the CMV enhanced chicken beta actin (CAG) promoter) (Fig.S1D). The monkey oocytes were obtained by super-ovulation and fertilized *in vitro* (IVF). The early-cleavage-stage embryos were injected with 50-100 pl lentivirus.

Totally, 5 pregnant surrogates produced 8 F0 monkeys (T_01-T_08), among which six of them are twins (T_01/T_02, T_03/T_04 and T_06/T_07) (Fig.1, Table 1). Caesarean section was used to deliver baby monkeys at around 155-days gestation except for the twins (T_03 and T_04) with premature abortion at embryonic 136 days. Multiple tissues (blood, placenta, umbilical cord endothelial cells and skin) were sampled to test the transgenic status, and all monkeys turned out to be positive (Fig. S1E-P). We detected strong GFP signals in the nucleus of the TG monkeys (Fig. S1P). Since *MCPH1* is known to work in nucleus [31], this result suggests that the huMCPH1 transgenes were correctly positioned in the cell.

To determine the integrated genomic locations and copy numbers, we conducted captured next-generation sequencing according to the reported method [32]. As expected for lentivirus, the huMCPH1 copies were randomly integrated into the monkey genomes. The eight TG monkeys have 2-9 huMCPH1 copies (Table 1 and Fig.1B). Importantly, all

integration sites are located in either inter-genic or non-coding regions and presumably will not interfere the function of the monkey endogenous genes (Table S1).

For comparison, we recruited 6 wild type (WT) monkeys (Fig.1C and Table S2), and initially they were divided into two groups. The first contained 3 age-matched monkeys (WT_01, WT_02 and WT_03) raised by their biological mothers. The second WT group contained 3 age-matched monkeys (WT_06, WT_07 and WT_08) who were separated from their biological mothers 6-25 days after birth and raised by humans under the same condition with the TG monkeys (Table S2). Unfortunately, TG_02 died of unknown cause at 76 days after birth. A biopsy did not reveal any organ damage. As mentioned above, TG_03 and TG_04 were abortions at embryonic 136 days. For comparison of brain tissue section and transcriptome analysis, six additional WT monkeys were sacrificed at the corresponding developmental stages (76 days after birth for WT_04 and WT_05, and embryonic 130-145 days for WT_09, WT_10, WT_11 and WT_12) (Table S2). In total, we collected data from 8 TG monkeys and 12 WT monkeys.

Brain development tracking using structural MRI suggests a delayed neural maturation

To test whether the integrated huMCPH1 copies influence brain development of the TG monkeys, we first performed a non-invasive analysis, *i.e.* structural magnetic resonance imaging (MRI) (Philips Achieva 3.0T TX). The tested monkeys included 5 TG monkeys (TG_01, TG_05, TG_06, TG_07 and TG_08) and 6 WT monkeys (WT_01, WT_02, WT_03, WT_06, WT_07 and WT_08). The MRI scans were conducted at scheduled intervals (once every month during 2-12 months old, and then once every 6 months till 2-3 years old) (Fig. 1C). Both T1-weighted image and diffusion tensor imaging (DTI) data were collected. Using the T1 image data, we calculated the volumes of total brain (TB), cerebellum, lobes and subcortical regions based on the published method and monkey atlas [33] (Fig.S2). To rule out the potential influence of feeding types, we first compared the two WT monkey groups (monkey feeding vs. human feeding), and we did not detect any difference in volumes (Table S3). Therefore, all WT monkeys were grouped together in the following analysis.

In general, the total brain volume and body weight of the TG monkeys were smaller than the WT monkeys during early development, likely due to C-section delivery of the TG monkeys at 155 days of pregnancy, about one-week earlier than natural delivery of the WT controls. Also, three of the five TG monkeys were twins which usually weight less than the single-birth monkeys (all WT monkeys were single-birth). However, this difference became smaller when the monkeys grew older and the TG monkeys eventually caught up with the WT monkeys at about three years old (Fig.S3A-B). Of note, the relative brain volume (TB volume adjusted by body weight) of the TG monkeys was larger than the WT monkeys during early postnatal development and this difference became invisible when the monkeys grew older (Fig.1D, LMM model, group effect p=0.05), while the cortex thickness was similar between them through development (Fig. 1E).

As the brain is mainly composed of cortex gray matter (GM, mostly neurons) and subcortical white matter (WM, mostly glial cells) [34], we next conducted segmentation analyses. Notably, during brain development, the cortex GM volume of the TG monkeys increased more slowly than the WT monkeys, and there was on average 164-days delay of peak time for the TG monkeys (Fig.1F). When the cortex was divided into four lobes (frontal, parietal, occipital and temporal lobes), we saw the same pattern in all lobes (Fig.S3C-F). Interestingly, the cortex GM ratios (the proportion of the GM volume vs. the total brain volume) of the TG monkeys were larger than those of the WT monkeys with a similar ratio peak time delay (Fig. 1F, LMM model, group effect p=0.06). By contrast, we did not detect such delay in cerebellum or subcortical region (Fig.S3G-H).

The developmental pattern of WM was different from GM. There were no volume/ratio peaks for the cortex WM, and the TG monkeys kept a significantly lower volume than the WT monkeys during development (Fig. 1G, LMM model, group effect p=0.0006), so did the cortex WM ratio (Fig. 1G, LMM model, group effect p=0.01). By contrast, the WM volume of subcortical region did not show such difference, and an opposite pattern was seen for cerebellum though statistically not significant (Fig.S3G-H, group effect p=0.59). Given the observed patterns, we reasoned that the observed brain developmental changes of the TG monkeys might reflect a delay of cortex development, rather than a developmental impairment. Consistent with this view, the cortex GM

volume curves of the TG and WT monkeys started to converge one year after birth (Fig. 1F), and the same pattern was observed when looking at the curves of the four lobes (Fig.S3C-F). In particular, TG_01 and three WT monkeys (WT_01, WT_02 and WT_03) had MRI data at later stages (~3 years old), and the cortex GM and WM volumes of TG_01 had already caught up with the WT monkeys (Fig. S4), supporting the proposed brain developmental delay.

To further explore brain developmental changes of the TG monkeys, we analyzed the MRI-DTI (diffusion tensor imaging) data to evaluate white matter properties, growth of brain structures and fiber tracts that connect them [35]. The fractional anisotropy (FA) index was used in characterizing degree of diffusion directionality and sensitive to axon size, density as well as degree of myelination [36]. Consistent with the observation of brain volume change, in three types of white matter tracts (projection fibers, association fiber and commissural fibers), the TG monkeys exhibited relatively lower FA values compared with the WT monkeys though statistically not significant (Fig.S5A-C and Fig.S6). The lower FA values suggest lower levels of myelination. Similar pattern was also observed when looking at the MD (mean diffusivity) values [37] (Fig.S7). Hence, the MRI-DTI data indicated a lower myelination level in the TG monkeys, implying a delayed neural fiber myelination and neural network maturation, which seem to mimic the known brain developmental delay (neoteny) of humans [38].

We also checked if there was a correlation between the number of the carried huMCPH1 copies and the brain structural measurements, and we did not find significant correlation with any measurements including total brain volume, cortex volume and cortex thickness etc (Fig.S8), suggesting that gene dosage effect is not obvious.

Brain tissue section analysis indicates delayed neuronal differentiation

To detect brain developmental changes at cellular level, we conducted brain tissue section analysis of the frontal lobe at both prenatal (2 TG and 4 WT monkeys at embryonic day-136) and postnatal (1 TG and 2 WT monkeys at 76 days after birth) stages (Fig.2A). Two marker genes were used to examine the status of neural cell proliferation and differentiation, including NeuN for matured neurons and GFAP for matured astrocytes. At prenatal stage (E136), there were 80% NeuN positive cells in the WT

monkeys, contrasting only 20% in TG_03 and 60% in TG_04 (p=1.25E-08, two-tailed t test; Fig. 2B). At postnatal stage (P76), 40%-60% cells were NeuN positive in the WT monkeys, but only 10% in TG_01 (p=6.0E-04, two-tailed t test; Fig. 2B). We detected similar ratio differences for astrocytes, with the WT monkeys having twice the ratio of GFAP positive cells as that of the TG monkeys (p<0.01, two-tailed t test; Fig. 2C).

The reduced ratios of matured neurons and astrocytes in the TG monkeys would predict elevated ratios of immature cells. To test this, we used two additional makers, *i.e.* DCX for immature neurons and FABP for immature astrocytes. As expected, the TG monkeys possessed much higher ratios of immature neurons and glia cells compared to the WT monkeys (p<0.001, two-tailed t test; Fig.2D-E). Of note, the total numbers of cells in the brain are similar between the TG monkeys and the WT monkeys (Fig.S9). Collectively, this cell-level difference is consistent with the observed myelination delay of the MRI data, as the fiber tracts are mostly composed of glial cells and myelinated nerve cells (axons).

Brain transcriptome analysis using bulk tissue

To gain insight into the molecular mechanism underling the speculated cortex developmental delay, we conducted RNAseq of the prefrontal cortex of the prenatal (2 TG vs 4 WT at E136) and postnatal monkeys (1 TG vs 2 WT at P76), with liver and muscle as the references. As expected, the overall *MCPH1* expression was much higher in the TG monkeys than in the WT monkeys for all tissue types, and the integrated huMCPH1 copies had much higher expression than the endogenous monkey MCPH1 (Fig.S10A, 11A). In the brain, there was a large number of differentially expressed genes (DEGs) between the TG and the WT monkeys (970 genes at embryonic day-136 and 1,933 genes at postnatal day-76) (Fig.S10B-C, 11B-C, TableS4). The numbers of DEGs were comparable in muscle and much less in liver. Only a small portion of DEGs were overlapped among tissues (Fig.S10D, 11D, TableS4), implying that the transgene huMCPH1 affects gene expression of the TG monkeys in a tissue-type-dependent manner.

To see functional enrichment of the DEGs in the brain, we performed GO ontology analysis using the ToppGene Suite [39]. At prenatal stage (E136), there were 350 significantly enriched functional categories for the TG-down-regulated genes (Table S5,

FDR B&H<0.05), and the top four categories were all related with synaptic signaling (Fig.S10E, left panel). In contrast, the enriched categories for the TG-up-regulated genes (60 categories, Table S6) were mostly basic cellular functions such as translation and protein localization to endoplasmic reticulum, not closely related with neural function (Fig.S10E, right panel). Similarly, at postnatal stage (P76), the top ten enriched categories for the TG-down-regulated genes were all related with neuron differentiation and neuron development, and synaptic signaling genes were also over-represented, while the top categories for the TG-up-regulated genes were mostly related with neuron projection (Fig.S11E and Table S7). The transcriptomic changes in the developing brains suggest that many neuron maturation and differentiation related genes were suppressed in the TG monkeys, consistent with the observed delay of neuron differentiation in tissue section analysis (Fig. 2).

Importantly, we found 107 brain DEGs shared between prenatal E136 and postnatal P76 stages (Fig. 3A). GO ontology analysis with these 107 genes indicated the highest enrichment category was synapse related function, confirming the observed pattern when using all brain DEGs (Fig.3B, 6/10). Remarkably, 35 of the 107 genes (32.7%) were overlapped with the known synapse genes in the datasets of *synaptome* [40] and *synsysnet* [41] (Fig.3C). Further analysis showed that about 50% of the 35 genes are either postsynapse- or synapse- related genes, and only 0.9% are presynapse related genes (Fig.3D). The hierarchical clustering analysis using the shared brain DEGs clearly distinguished the TG and the WT monkeys with the most prominent distinction between brain and muscle/liver (Fig.3E). For example, *NR4A1* is a downstream gene of *MEF2A*, a gene playing a critical role in activity-induced synaptic modification [42]. This gene showed 76% (at E136) and 26% (at P76) expression reduction in the TG monkeys. In the mouse model, overexpression of *NR4A1* would eliminate dendritic spines while knockdown of *NR4A1* could cause excessive number of spines and major postsynaptic density [43]. Together, these data suggest that at bulk tissue level, the transgene huMCPH1 mainly suppress expression of neural differentiation and synapse function related genes.

Generation of F1 TG monkeys and transcriptome analysis of fetal cortical lamina

To further dissect the impact of the huMCPH1 copies on brain development, we generated three F1 TG monkeys by IVF using the sperms of TG_01 that we proved carrying the huMCPH1 copies in the germ line (Fig.S12). The three F1 TG monkeys were sacrificed at embryonic day-76 (TG_09 at E76) and embryonic day-92 (TG_10 and TG_11 at E92), the two developmental time points during neurogenesis peak in rhesus monkeys [44]. Captured sequencing analysis indicated that the three F2 TG monkeys all carried the huMCPH1 copies at the same integrated sites with TG_01 (Table S1). With the use of IVF, we also obtained 5 WT fetal monkeys at the corresponding developmental points (2 WT at E76 and 3 WT at E92, Table S2). To conduct more detailed developmental tracking, we sampled the frontal cortex and dissected (using laser micro-dissection) the brain tissue into four cortical laminae as they reflect different stages of neural proliferation, differentiation and migration, including cortical plate (CP), outer subventricular zone (OSVZ), subventricular zone (SVZ) and ventricular zone (VZ) (Fig.4A). RNAseq was performed for each lamina.

Firstly, we checked *MCPH1* expression in WT monkey embryos and we found that at E76, no difference existed between CP and germinal zone (OSVZ, SVZ and VZ), while at E92, *MCPH1* expression is higher in germinal zone than in CP, consistent with the reported pattern in mouse [24] (Fig.S13A). As expected, in the TG monkey embryos, the transgene huMCPH1 had a much higher expression than the endogenous *MCPH1* in all laminae at both E76 and E92 (Fig.S13B). The fold changes were different among different laminae. SVZ had the highest fold change at E76, while CP had the highest fold change at E92 (Fig.S13B).

The principal component analysis (PCA) showed that the RNA profiles can distinguish different developmental cortical laminae. VZ and CP were clearly separated as they represent undifferentiated neuro-progenitors and differentiated neural cells, respectively, while the separation between SVZ and OSVZ was incomplete because they are the intermediate stages in view of cell proliferation, migration and differentiation (Fig.4A). Consistently, the marker genes for neuro-progenitors (*SOX2*) and neurons (*SYT1*) showed expected expression pattern in these laminae (Fig.4A). We then analyzed DEGs of the four laminae between the TG monkeys and the WT monkeys. As expected, the transgene

huMCPH1 caused expression changes of many genes, and this pattern was more pronounced at E92 compared to E76 (140-350 genes for E76 and 3000-9000 genes for E92, Table S8) (Fig.S13 C-D). The GO ontology analysis showed that at E76, there were 25 enriched categories for CP, 26 for OSVZ, 41 for SVZ and 10 for VZ (Table S9-12, FDR B&H <0.05). Among the top 10 categories, the enriched functional terms were cell development (CP, 5/10), synapse signaling (OSVZ, 5/10), cell differentiation and proliferation (SVZ, 5/10) and cilium function (VZ, 3/10) (Fig.S13E, left panel, FDR B&H <0.05). In contrast, there were a lot more enriched categories at E92 (453 for CP, 109 for OSVZ, 102 for SVZ and 786 for VZ (Table S13-16, FDR B&H <0.05), among which the top categories were mRNA catabolic process (CP, 3/10), neuron differentiation, neurogenesis and cell migration (OSVZ, 5/10), cell cycle and mRNA processing (SVZ, 10/10), and immune response (VZ, 8/10) (Fig.S13E, right panel, FDR B&H <0.05).

We next conducted lamina to lamina pairwise comparisons in the TG and the WT monkeys separately. Markedly, at E76, the TG monkeys exhibited much less between-lamina expression difference than the WT monkeys. In particular, there were no DEGs when comparing SVZ with OSVZ in the TG monkeys, contrasting 557 DEGs in the WT monkeys (Fig.4B, Table S17). A similar pattern was seen at E92. For example, there were 61 CP vs OSVZ DEGs in the TG monkeys, while there were 9,186 DEGs in the WT monkeys (Fig.4C, Table S18). This result suggests that cortical lamina distinction is much weaker for the TG monkeys compared to the WT monkeys, supporting the proposed delay of neuronal maturation and differentiation. Consistently, we observed delayed expression peaks of four known neuron differentiation markers, including *SYP* (Synaptic vesicle protein p38), *ENO2* (Cytosolic protein t), *GAD1* (Glutamic acid decarboxylase) and *MAP2* (Cytoskeletal protein) (Fig.4D).

Furthermore, in order to see the temporal pattern of gene expression delay in the TG monkeys, we combined the RNAseq data of all four developmental stages, including E76, E92, E136 and P76 (6 TG vs 11 WT). We classified those genes showing expression delay in the TG monkeys into three types according to their expression peak times in the WT monkeys (Fig.S14A-B). The Type-1 genes are those with an expression peak shift from E92 in the WT monkeys to E136 in the TG monkeys (*e.g.* the *SLC44A2* gene). The

Type-2 genes had a peak shift from E136 in the WT monkeys to P76 in the TG monkeys (*e.g.* the *SYP* gene), while the Type-3 genes had a peak shift from E92 in the WT monkeys to P76 in the TG monkeys (*e.g.* the *CDK5* gene) (Fig.S14A). In total, we identified 185, 347 and 50 genes for Tyep-1, Type-2 and Type-3 delays, respectively (Fig.S14B). We then performed GO ontology analysis and only the Type-2 genes showed significant enrichment of functional categories, implying that the developmental stage close to birth was the most affected in the TG monkeys. Consistent with the results of bulk tissue RNAseq, the Type-2 genes from cortical laminae containing undifferentiated cells (VZ, SVZ and OSVZ) were mainly enriched for synapse related functions such as trans-synapse signaling, chemical synapse transmission and synaptic signaling (Fig.S14C, p <0.001), and the involved genes showed delayed expression peaks at P76 or later stages in the TG monkeys.

To test whether the observed gene expression delay in the TG monkeys show human-like features, we obtained data from a previous study in which genes with human-specific expression delay were identified by comparing postnatal brain development in the prefrontal cortex of humans, chimpanzees, and rhesus macaques [11]. We found that only the Type-2 genes were enriched in the reported Module-I gene set with human-specific expression delay (p<0.0001; hypergeometric test; Fig.S14D and Table S19). For example, *MEF2A* is a Type-2 gene and also a Module-I gene, which not only plays a role in neuron differentiation [45], but also mediates a human-specific time shift of cortex synaptic development [11]. Hence, the patterns of gene expression delay are consistent between the data from the bulk tissue and the data for the laminae, and many neural-differentiation-related genes were suppressed in the TG monkeys with human-like expression delays during brain development.

General behavior analysis and test of short-term memory

To test whether the observed brain developmental delay at molecular and cellular levels in the TG monkeys can be transformed into cognitive changes, we first performed an analysis of general behaviors (4 TG vs. 4 WT age-matched monkeys during 24-36 months old; see Methods for details). A total of 9 indexes for general behaviors were measured [46], including self-injury behavior, stereotypical behavior, feeding, self-grooming, locomotion, resting, bouts of waken, waken and sleep. No difference was

detected between the TG and the WT monkeys, suggesting that the transgene huMCPH1 did not cause abnormal behaviors in the TG monkeys (Fig.S15).

Next, we performed a test of short-term memory using the delayed matching to sample (DMS) task, which was known correlated with prefrontal cortex function [47-49]. The computerized touch-screen behavioral battery (Cambridge Neuropsychological Test Automated Batteries, CANTAB; Lafayette, USA) was used. The DMS task requires the monkeys to remember the color and the shape of a stimuli on the screen for a specified delayed time. The monkeys were initially habituated in testing room for 5 days and then subject to touch traing. Touch training was divided into two phases. In Phase-1, monkeys were subject to touch training for continuous 15 days. In Phase-2, monkeys were required to have >85% correction rate for 3 continuous days in the training sessions and then were subject to DMS task test (Fig. 5A, Fig.S16 and Supplementary Video 1; more details about touch training is provided in the methods). The results showed that at 0~4sec delayed times, the TG monkeys performed significantly better than the WT monkeys (Fig. 5B, GLM model , group effect p=0.0086), and this difference became more pronounced in the sessions with 8sec and 16sec delayed times (Fig. 5B; GLM model, 8s, group effect p= 0.0022; 16s, group effect p=5.5E-04). When the delayed time extended to 32sec, the difference remained (Fig.5B, GLM model, group effect p=0.032). When all sessions with different delayed times were combined together, the TG monkeys had a significantly better performance than the WT monkeys (Fig.5B, GLM model, group effect p=7.5E-04). Interestingly, we also observed significantly shorter reaction times (response latency) in the TG monkeys for all categories of delayed times (p<0.001, two-tailed t test, Fig.5B). Collectively, the TG monkeys exhibited better performance in the DMS task than the WT monkeys, suggesting that the brain developmental delay caused by the transgene huMCPH1 may enhance short-term memory of the TG monkeys.

Discussion

MCPH1 is one of the strong candidates for human brain evolution since it has accumulated human-specific protein sequence and gene expression changes [17, 18]. Ideally, a gene replacement model would be preferred so that the influence of the endogenous monkey *MCPH1* could be removed. However, due to the long generation time of monkeys (4-5 years), current gene editing tools are still impractical in generating

such a model in monkeys. We argue that a transgenic monkey model is practical and to a large extend can mimic the human-specific status. The transgenic monkeys carry the human *MCPH1* copies so that the effect of the human-specific protein sequence changes can be tested. At the same time, since the transgenic monkeys overexpress the huMCPH1 transgene, and this can mimic the human-specific increase of gene expression.

Because *MCPH1* is a key gene for neurogenesis, one of the expected phenotypic outcomes in the transgenic monkeys would be a larger brain, which was not the case in this study. We showed that the TG monkeys carrying the huMCPH1 transgene did not manifest an enlarged brain size, implying that a single gene likely has limited effect on neural progenitor pool proliferation during brain development. Alternatively, it is equally possible that the human-specific changes of *MCPH1* may not enhance its known function in neuro-progenitor proliferation [22], rather they work on the unknown function of *MCPH1* in neuronal maturation, neural plasticity and synapse signaling, which were supported by multiple lines of evidence presented in this study.

Our analyses found a developmental delay of gray matter in the brain of the TG monkeys, suggesting that the huMCPH1 transgene may delay neuron differentiation and maturation during brain development. Consistent with the cortex developmental delay, there were much less mature neurons and glia cells in the TG monkeys compared to the WT monkeys during early period of postnatal development. Consistently, the tissue-level transcriptome comparisons indicated a large number of neuron differentiation, development and synapse genes were suppressed in the TG monkeys, providing a possible molecular basis for the observed delay of cell maturation and fiber myelination in the brain. In fact, our previous *in vitro* experiments demonstrated that MCPH1 can act as a transcription repressor and repress telomerase activity [50]. Furthermore, the cortical-lamina transcriptome comparisons showed that the huMCPH1 transgene can influence gene expression at all laminae including CP, OSVZ, SVZ and VZ as early as prenatal E76, indicating that the huMCPH1 transgene may alter neurogenesis by affecting neuro-progenitor cell division and differentiation. In fact, previous mouse study already showed that MCPH1 is required for precisely mitotic spindle orientation during neurogenesis [22]. Additionally, as expected, cortical lamina pairwise comparisons suggested that the between-laminae differences in the TG monkeys were not as obvious

as in the WT monkeys, consistent with the proposed delay of neural differentiation. Hence, the huMCPH1 transgene may contribute to delaying cortical lamina differentiation in the TG monkeys. Taken together, we propose that overexpression of the huMCPH1 transgene can cause neural developmental delay due to the down-regulation of many neural differentiation related genes. Future experiments are warranted to reveal the detailed molecular pathways.

One hallmark difference between humans and nonhuman primates is that humans require a much longer time to shape their neuro-networks during development, greatly elongating the childhood, *i.e.* the so-called "neoteny". Myelination is the process of generating myelin sheaths around nerve fibers so that neural signals can be propagated more swiftly with less signal loss. This process is considered a key developmental aspect of the human brain, and continues at least 10-12 years after birth, providing an extended window of neural network plasticity [51]. In fact, human neocortical myelination is developmentally protracted compared with chimpanzees [52]. We speculate that the observed neural maturation delay in the TG monkeys may extend their time window of neural network plasticity, similar to the brain developmental neoteny of humans. In support of our speculation, when we combined the RNAseq data of all developmental stages, we found that many of the delay genes were synapse related genes, which are required for experience-dependent process of neural network plasticity [53]. More interestingly, most of the delay genes showed human-specific changes in timing of synaptic development in the previous study [11]. For example, *MEF2A* and *SYP* were among the key genes showing human-specific delay of youth-like expression compared with chimpanzee and macaque [11]. Notably, synapse and spine density in the human projection neurons is much higher than that in rhesus macaque, which is associated with the higher cognitive performance in humans [11, 54].

The speculated extension of neural network plasticity in the TG monkeys gained further support from our preliminary cognitive data. The TG monkeys showed an improved short-term memory, suggesting that the observed brain developmental delay in the TG monkeys is beneficial possibly through extending the time window of neural network plasticity. More interestingly, the TG monkeys displayed a significantly shorter reaction time than the WT monkeys during the DMS task, which is another hint of

cognitive improvement. More sophisticated cognitive tests are needed to understand the long-term effect of the huMCPH1 transgene in the TG monkeys.

Our findings demonstrated that transgenic nonhuman primates (excluding ape species) have the potential to provide important—and potentially unique—insights into basic questions of what actually makes human unique, as well as into disorders and clinically relevant phenotypes, such as neurodegenerative and social behavior disorders that are difficult to study by other means [32, 46, 55]. But such gains must invariably be weighed against potential ethical concerns [29, 56, 57]. We noted that the transgenic monkey model also has limitations, including the influence of the endogenous monkey gene copy and the incapability to differentiate the effects of protein sequence changes from gene expression changes. Several recent technical improvements (*e.g.* CRISPR-Cas9) have shown the hope of conducting precision genome editing in monkeys [26, 58-61], providing more powerful tools to future studies on understanding the genetic basis of human brain evolution.

METHODS

The detailed methods and materials are available as Supplementary Data at NSR online.

acknowledgments

The wild-type MCPH1 plasmid was kindly provided by Prof. Xingzhi Xu (Capital Normal University, China). We are grateful to Prof. Xintian Hu and Drs. Dongdong Qin and Shihao Wu for their advice on behavioral and cognitive tests. The monkey icon in Fig.5 was obtained using Freepick at www.flaticon.com. We thank Hui Zhang and Yan Guo for their technical assistance in this study.

Funding

This study was supported by the Strategic Priority Research Program of the Chinese Academy of Sciences (XDB13000000 to B.S), the National Natural Science Foundation of China (31730088 and 31621062 to B.S) and the Youth Innovation Promotion Association of CAS [to L.S].

Author Contributions

L.S. and B.S., designed the study; L.S., X.L, J.J, T.L, M.L. and Q.L performed the experiments; H.W., contributed to animal care and management; CR. L, JH, W. assisted

the MRI image data analysis; Y.N., X.H., Y.C., W.J., assisted in monkey reproductive technique and virus gene transfer; L.S., X.L, Y.L., YY. M., X. S., H. Y., conducted MRI scanning; Y. L, T. L, assisted the histological studies; L.S, B.S., performed data analysis; L.S., X.L, J.J and B.S., wrote the manuscript.

Conflict interest

The authors declare no conflict interest.

References

1. Clark AG, Glanowski S, Nielsen R, et al.; Inferring nonneutral evolution from human-chimp-mouse orthologous gene trios. *Science* 2003;**302**(5652):1960-3. doi: 10.1126/science.1088821.
2. Bustamante CD, Fledel-Alon A, Williamson S, et al.; Natural selection on protein-coding genes in the human genome. *Nature* 2005;**437**(7062):1153-1157. doi: Doi 10.1038/Nature04240.
3. Necsulea A, Soumillon M, Warnefors M, et al.; The evolution of lncRNA repertoires and expression patterns in tetrapods. *Nature* 2014;**505**(7485):635-40. doi: 10.1038/nature12943.
4. Bentwich I, Avniel A, Karov Y, et al.; Identification of hundreds of conserved and nonconserved human microRNAs. *Nat Genet* 2005;**37**(7):766-70. doi: 10.1038/ng1590.
5. Zhang R, Peng Y, Wang W, et al.; Rapid evolution of an X-linked microRNA cluster in primates. *Genome Res* 2007;**17**(5):612-7. doi: 10.1101/gr.6146507.
6. Bailey JA, Gu ZP, Clark RA, et al.; Recent segmental duplications in the human genome. *Science* 2002;**297**(5583):1003-1007. doi: DOI 10.1126/science.1072047.
7. Dennis MY, Nuttle X, Sudmant PH, et al.; Evolution of Human-Specific Neural SRGAP2 Genes by Incomplete Segmental Duplication. *Cell* 2012;**149**(4). doi: DOI 10.1016/j.cell.2012.03.033.
8. Florio M, Albert M, Taverna E, et al.; Human-specific gene ARHGAP11B promotes basal progenitor amplification and neocortex expansion. *Science* 2015;**347**(6229):1465-70. doi: 10.1126/science.aaa1975.
9. Khaitovich P, Hellmann I, Enard W, et al.; Parallel patterns of evolution in the genomes and transcriptomes of humans and chimpanzees. *Science* 2005;**309**(5742):1850-1854. doi: DOI 10.1126/science.1108296.
10. Enard W, Khaitovich P, Klose J, et al.; Intra- and interspecific variation in primate gene expression patterns. *Science* 2002;**296**(5566):340-343. doi: DOI 10.1126/science.1068996.
11. Liu X, Somel M, Tang L, et al.; Extension of cortical synaptic development distinguishes humans from chimpanzees and macaques. *Genome Res* 2012;**22**(4):611-22. doi: 10.1101/gr.127324.111.
12. He Z, Han D, Efimova O, et al.; Comprehensive transcriptome analysis of neocortical layers in humans, chimpanzees and macaques. *Nat Neurosci* 2017. doi: 10.1038/nn.4548.
13. Zeng J, Konopka G, Hunt BG, et al.; Divergent Whole-Genome Methylation Maps of Human and Chimpanzee Brains Reveal Epigenetic Basis of Human Regulatory Evolution. *American Journal of Human Genetics* 2012;**91**(3):455-465. doi: DOI 10.1016/j.ajhg.2012.07.024.
14. Shulha HP, Crisci JL, Reshetov D, et al.; Human-specific histone methylation signatures at transcription start sites in prefrontal neurons. *PLoS Biol* 2012;**10**(11):e1001427. doi: 10.1371/journal.pbio.1001427.
15. Mendizabal I, Shi L, Keller TE, et al.; Comparative Methylome Analyses Identify Epigenetic Regulatory Loci of Human Brain Evolution. *Mol Biol Evol* 2016;**33**(11):2947-2959. doi: 10.1093/molbev/msw176.
16. Pulyers JN, Journiac N, Arai Y, et al.; MCPH1: a window into brain development and evolution. *Frontiers in Cellular Neuroscience* 2015;**9**. doi: ARTN 92
10.3389/fncel.2015.00092.
17. Wang YQ, Su B; Molecular evolution of microcephalin, a gene determining human brain size. *Hum Mol Genet* 2004;**13**(11):1131-7. doi: 10.1093/hmg/ddh127
ddh127 [pii].

18. Shi L, Li M, Lin Q, et al.; Functional divergence of the brain-size regulating gene MCPH1 during primate evolution and the origin of humans. *BMC Biol* 2013;**11**:62. doi: 10.1186/1741-7007-11-62.
19. Yang S-Z, Lin F-T, Lin W-C; MCPH1/BRIT1 cooperates with E2F1 in the activation of checkpoint, DNA repair and apoptosis. *EMBO Rep* 2008;**9**(9):907-915.
20. Liu X, Zhou ZW, Wang ZQ; The DNA damage response molecule MCPH1 in brain development and beyond. *Acta Biochim Biophys Sin (Shanghai)* 2016;**48**(7):678-85. doi: 10.1093/abbs/gmw048.
21. Peng G, Yim EK, Dai H, et al.; BRIT1/MCPH1 links chromatin remodelling to DNA damage response. *Nat Cell Biol* 2009;**11**(7):865-72. doi: ncb1895 [pii]
10.1038/ncb1895.
22. Gruber R, Zhou Z, Sukchev M, et al.; MCPH1 regulates the neuroprogenitor division mode by coupling the centrosomal cycle with mitotic entry through the Chk1-Cdc25 pathway. *Nat Cell Biol* 2011. doi: ncb2342 [pii]
10.1038/ncb2342.
23. Woods CG, Bond J, Enard W; Autosomal recessive primary microcephaly (MCPH): a review of clinical, molecular, and evolutionary findings. *Am J Hum Genet* 2005;**76**(5):717-28. doi: 10.1086/429930.
24. Jackson AP, Eastwood H, Bell SM, et al.; Identification of Microcephalin, a Protein Implicated in Determining the Size of the Human Brain. *Am.J.Hum.Genet* 2002;**71**(1):136-142.
25. Trimborn M, Bell SM, Felix C, et al.; Mutations in Microcephalin Cause Aberrant Regulation of Chromosome Condensation. *American journal of human genetics* 2004;**75**(2):261-266.
26. Ke Q, Li W, Lai X, et al.; TALEN-based generation of a cynomolgus monkey disease model for human microcephaly. *Cell Res* 2016;**26**(9):1048-61. doi: 10.1038/cr.2016.93.
27. Zhong S, Zhang S, Fan X, et al.; A single-cell RNA-seq survey of the developmental landscape of the human prefrontal cortex. *Nature* 2018;**555**(7697):524-528. doi: 10.1038/nature25980.
28. Yan G, Zhang G, Fang X, et al.; Genome sequencing and comparison of two nonhuman primate animal models, the cynomolgus and Chinese rhesus macaques. *Nat Biotechnol* 2011;**29**(11):1019-23. doi: 10.1038/nbt.1992.
29. Coors ME, Glover JJ, Juengst ET, et al.; SCIENCE AND SOCIETY The ethics of using transgenic non-human primates to study what makes us human. *Nature Reviews Genetics* 2010;**11**(9):658-662. doi: Doi 10.1038/Nrg2864.
30. Shi L, Su B; Identification and functional characterization of a primate-specific E2F1 binding motif regulating MCPH1 expression. *FEBS J* 2012;**279**(3):491-503. doi: 10.1111/j.1742-4658.2011.08441.x.
31. Xu X, Lee J, Stern DF; Microcephalin Is a DNA Damage Response Protein Involved in Regulation of CHK1 and BRCA1. *J Biol Chem* 2004;**279**(33):34091-34094. doi: 10.1074/jbc.C400139200.
32. Liu Z, Li X, Zhang JT, et al.; Autism-like behaviours and germline transmission in transgenic monkeys overexpressing MeCP2. *Nature* 2016;**530**(7588):98-102. doi: 10.1038/nature16533.
33. Liu C, Tian X, Liu H, et al.; Rhesus monkey brain development during late infancy and the effect of phencyclidine: a longitudinal MRI and DTI study. *Neuroimage* 2015;**107**:65-75. doi: 10.1016/j.neuroimage.2014.11.056.
34. Hofman MA; Size and Shape of the Cerebral-Cortex in Mammals .1. The Cortical Surface. *Brain Behavior and Evolution* 1985;**27**(1):28-40. doi: Doi 10.1159/000118718.
35. Mori S, Zhang J; Principles of diffusion tensor imaging and its applications to basic neuroscience research. *Neuron* 2006;**51**(5):527-39. doi: 10.1016/j.neuron.2006.08.012.
36. Pierpaoli C, Basser PJ; Toward a quantitative assessment of diffusion anisotropy. *Magnetic Resonance in Medicine* 1996;**36**(6):893-906. doi: DOI 10.1002/mrm.1910360612.
37. Madden DJ, Bennett IJ, Burzynska A, et al.; Diffusion tensor imaging of cerebral white matter integrity in cognitive aging. *Biochim Biophys Acta* 2012;**1822**(3):386-400. doi: 10.1016/j.bbadis.2011.08.003.
38. Montagu MFA; Time, Morphology, and Neoteny in the Evolution of Man. *American Anthropologist* 1955;**57**(1):13-27. doi: DOI 10.1525/aa.1955.57.1.02a00030.
39. Huang da W, Sherman BT, Lempicki RA; Bioinformatics enrichment tools: paths toward the comprehensive functional analysis of large gene lists. *Nucleic Acids Res* 2009;**37**(1):1-13. doi: 10.1093/nar/gkn923.
40. Pirooznia M, Wang T, Avramopoulos D, et al.; SynaptomeDB: an ontology-based knowledgebase

for synaptic genes. *Bioinformatics* 2012;**28**(6):897-9. doi: 10.1093/bioinformatics/bts040.
41. von Eichborn J, Dunkel M, Gohlke BO, et al.; SynSysNet: integration of experimental data on synaptic protein-protein interactions with drug-target relations. *Nucleic Acids Res* 2013;**41**(Database issue):D834-40. doi: 10.1093/nar/gks1040.
42. Hawk JD, Abel T; The role of NR4A transcription factors in memory formation. *Brain Res Bull* 2011;**85**(1-2):21-9. doi: 10.1016/j.brainresbull.2011.02.001.
43. Chen Y, Wang Y, Erturk A, et al.; Activity-induced Nr4a1 regulates spine density and distribution pattern of excitatory synapses in pyramidal neurons. *Neuron* 2014;**83**(2):431-443. doi: 10.1016/j.neuron.2014.05.027.
44. Betizeau M, Cortay V, Patti D, et al.; Precursor diversity and complexity of lineage relationships in the outer subventricular zone of the primate. *Neuron* 2013;**80**(2):442-57. doi: 10.1016/j.neuron.2013.09.032.
45. Zhu B, Carmichael RE, Solabre Valois L, et al.; The transcription factor MEF2A plays a key role in the differentiation/maturation of rat neural stem cells into neurons. *Biochem Biophys Res Commun* 2018;**500**(3):645-649. doi: 10.1016/j.bbrc.2018.04.125.
46. Chen Y, Yu J, Niu Y, et al.; Modeling Rett Syndrome Using TALEN-Edited MECP2 Mutant Cynomolgus Monkeys. *Cell* 2017;**169**(5):945-955 e10. doi: 10.1016/j.cell.2017.04.035.
47. Fuster JM, Alexander GE; Neuron activity related to short-term memory. *Science* 1971;**173**(3997):652-4.
48. Carlen M; What constitutes the prefrontal cortex? *Science* 2017;**358**(6362):478-+. doi: 10.1126/science.aan8868.
49. Goldman-Rakic PS; Cellular basis of working memory. *Neuron* 1995;**14**(3):477-85.
50. Shi L, Li M, Su B; MCPH1/BRIT1 represses transcription of the human telomerase reverse transcriptase gene. *Gene* 2012;**495**(1):1-9. doi: S0378-1119(11)00837-7 [pii]
10.1016/j.gene.2011.12.053.
51. Paus T, Zijdenbos A, Worsley K, et al.; Structural maturation of neural pathways in children and adolescents: In vivo study. *Science* 1999;**283**(5409):1908-1911. doi: DOI 10.1126/science.283.5409.1908.
52. Miller DJ, Duka T, Stimpson CD, et al.; Prolonged myelination in human neocortical evolution. *Proc Natl Acad Sci U S A* 2012;**109**(41):16480-5. doi: 10.1073/pnas.1117943109.
53. West AE, Greenberg ME; Neuronal activity-regulated gene transcription in synapse development and cognitive function. *Cold Spring Harb Perspect Biol* 2011;**3**(6). doi: 10.1101/cshperspect.a005744.
54. Duan H, Wearne SL, Rocher AB, et al.; Age-related dendritic and spine changes in corticocortically projecting neurons in macaque monkeys. *Cereb Cortex* 2003;**13**(9):950-61.
55. Yang SH, Cheng PH, Banta H, et al.; Towards a transgenic model of Huntington's disease in a non-human primate. *Nature* 2008;**453**(7197):921-U56. doi: 10.1038/nature06975.
56. Jennings CG, Landman R, Zhou Y, et al.; Opportunities and challenges in modeling human brain disorders in transgenic primates. *Nat Neurosci* 2016;**19**(9):1123-30. doi: 10.1038/nn.4362.
57. Izpisua Belmonte JC, Callaway EM, Caddick SJ, et al.; Brains, genes, and primates. *Neuron* 2015;**86**(3):617-31. doi: 10.1016/j.neuron.2015.03.021.
58. Niu Y, Shen B, Cui Y, et al.; Generation of gene-modified cynomolgus monkey via Cas9/RNA-mediated gene targeting in one-cell embryos. *Cell* 2014;**156**(4):836-43. doi: 10.1016/j.cell.2014.01.027.
59. Liu H, Chen Y, Niu Y, et al.; TALEN-mediated gene mutagenesis in rhesus and cynomolgus monkeys. *Cell Stem Cell* 2014;**14**(3):323-8. doi: 10.1016/j.stem.2014.01.018.
60. Liu Z, Cai Y, Liao Z, et al.; Cloning of a gene-edited macaque monkey by somatic cell nuclear transfer. *National Science Review* 2019;**6**(1):101-108. doi: 10.1093/nsr/nwz003.
61. Qiu P, Jiang J, Liu Z, et al.; BMAL1 knockout macaque monkeys display reduced sleep and psychiatric disorders. *National Science Review* 2019;**6**(1):87-100. doi: 10.1093/nsr/nwz002.

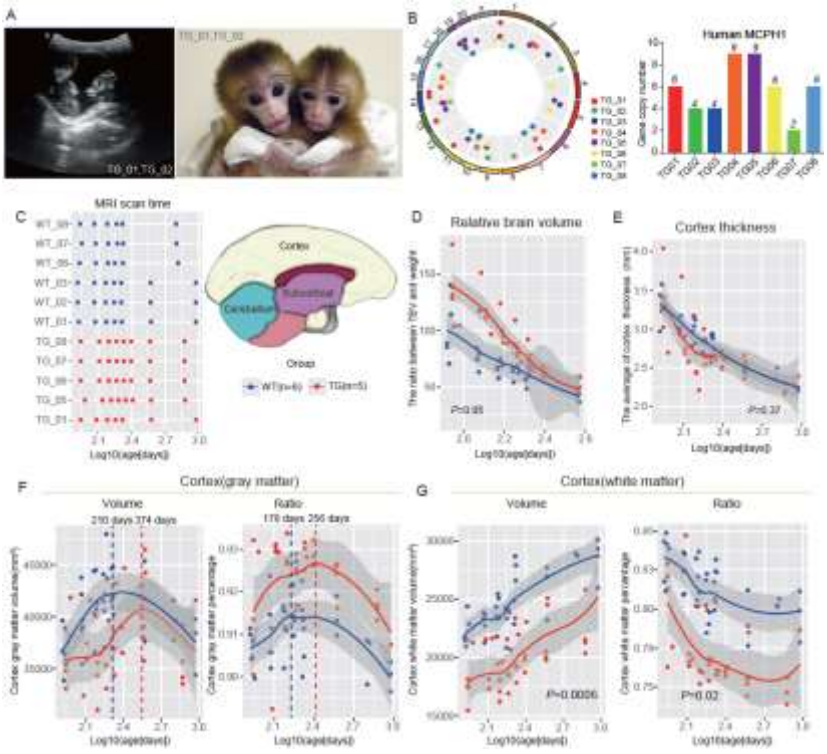

Figure 1. Brain developmental tracking of the TG monkeys via structural MRI. (A) Left panel: the ultrasound image showing the twin monkeys (TG_01 and TG_02) at 58 days of gestation; Right panel: the newborn twin TG monkeys: TG_01 (male, left) and TG_02 (female, right). (B) Left panel: Genomic distribution of the huMCPH1 transgene copies in the TG monkeys. The transgene insertion sites (dots) are randomly distributed on the chromosomes (outermost circle). Right panel: Bar plot of the huMCPH1 copy numbers in the TG monkeys. (C) Left panel: the time points (log10(age-days)) of MRI scans of the 5 TG and 6 WT monkeys, with the first scan at about 2 months after birth and the last scan at 2-3 years old. Right panel: the schematic map of brain regions. (D) The change of relative brain volume (measured by the total brain volume divided by body weight) during development. (E) The change of cortex thickness during development. (F) The change of cortex gray matter volume and ratio during brain development. (G) The change of cortex white matter volume and ratio during brain development. Group effect P value was calculated based on LMM (linear mixed model), and $P<0.05$ was taken as statistically significant. The dashed vertical lines indicate the peaks of cortex gray matter volumes or ratios.

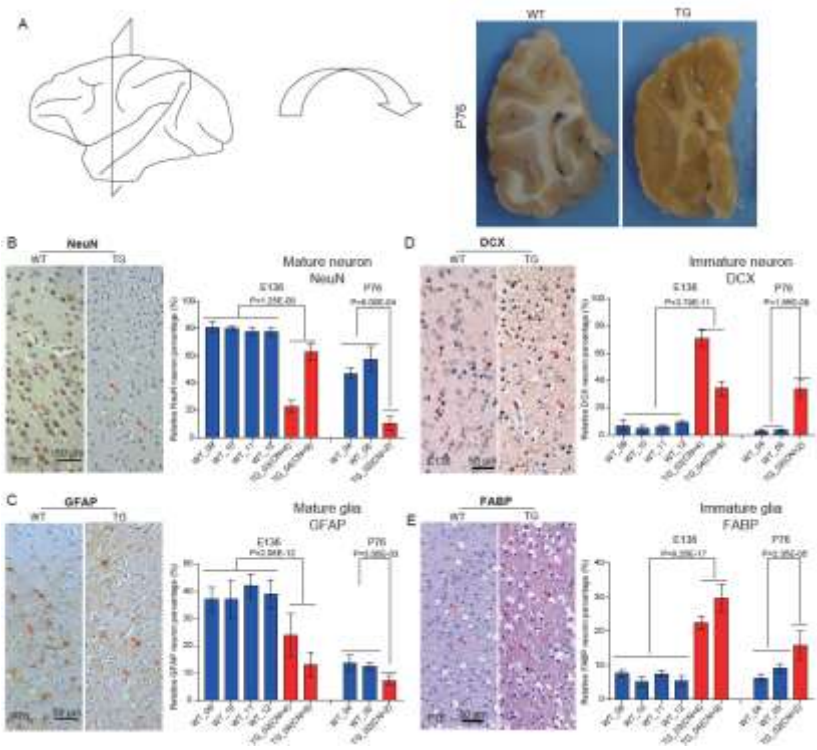

Figure 2. Brain immunohistochemistry analysis with gene markers. (A) The schematic indication of the sampled frontal lobe region of the P76 monkey brain. (B) Immunohistochemical staining of NeuN, the marker gene for matured neurons. Quantification of the NeuN positive neurons indicates fewer matured neurons in the TG monkeys compared with the WT monkeys. (C) Immunohistochemical staining of GFAP, the marker gene for matured astrocytes; Quantification of the GFAP positive astrocytes indicates decreased mature astrocytes in the TG monkeys. (D) Immunohistochemical staining of DCX, the marker gene for immature neurons. Quantification of the DCX positive neurons indicates more immature neurons in the TG monkeys. (E) Immunohistochemical staining of FABP, the marker gene for immature astrocytes. Quantification of the FABP positive astrocytes indicates more immature astrocytes in the TG monkeys. All histograms represent the mean ± SD of at least two sections and each section include counts of four different visual fields. The red arrows indicate positively stained cells. The two-tailed unpaired t-test was used for statistical assessment and CN stands for copy number.

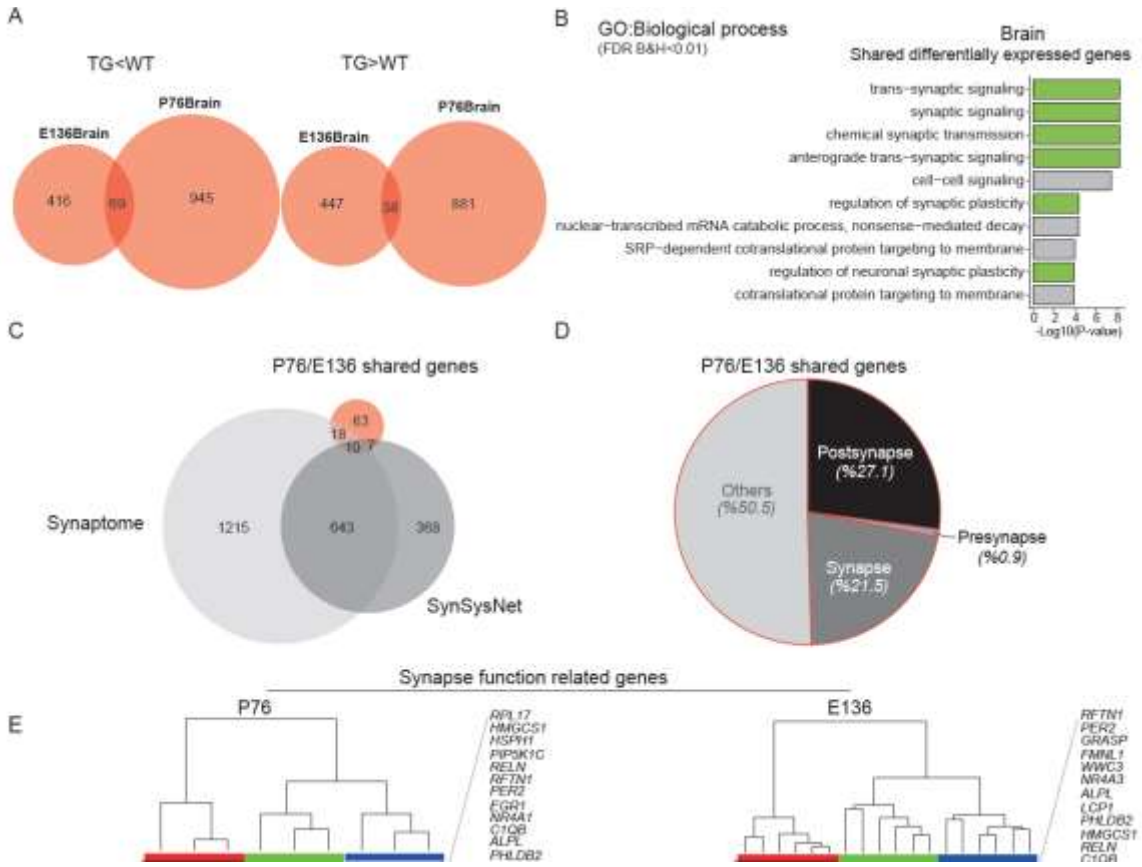

Figure 3. Brain transcriptome analysis at prenatal E136 and postnatal P76. (A) The Venn diagrams showing overlaps among differentially expressed genes (DEGs, TG vs. WT) in the brain between E136 and P76. (B) Enriched gene clusters of DEGs in the brain. The green blocks indicate synapse signaling associated clusters. (C) The Venn diagrams showing overlaps among the E136/P76 shared genes, the synaptome genes and the synsysnet genes. The hypergeometric tests indicate significant overlaps with the synaptome genes (P=4.89E-08) and with the synsysnet genes (P=7.74E-06). (D) The pie chart of the E136/P76 shared genes indicates about 50% of the genes are synapse and post-synapse related genes. (E) The hierarchical clustering using the E136/P76 shared brain DEGs.

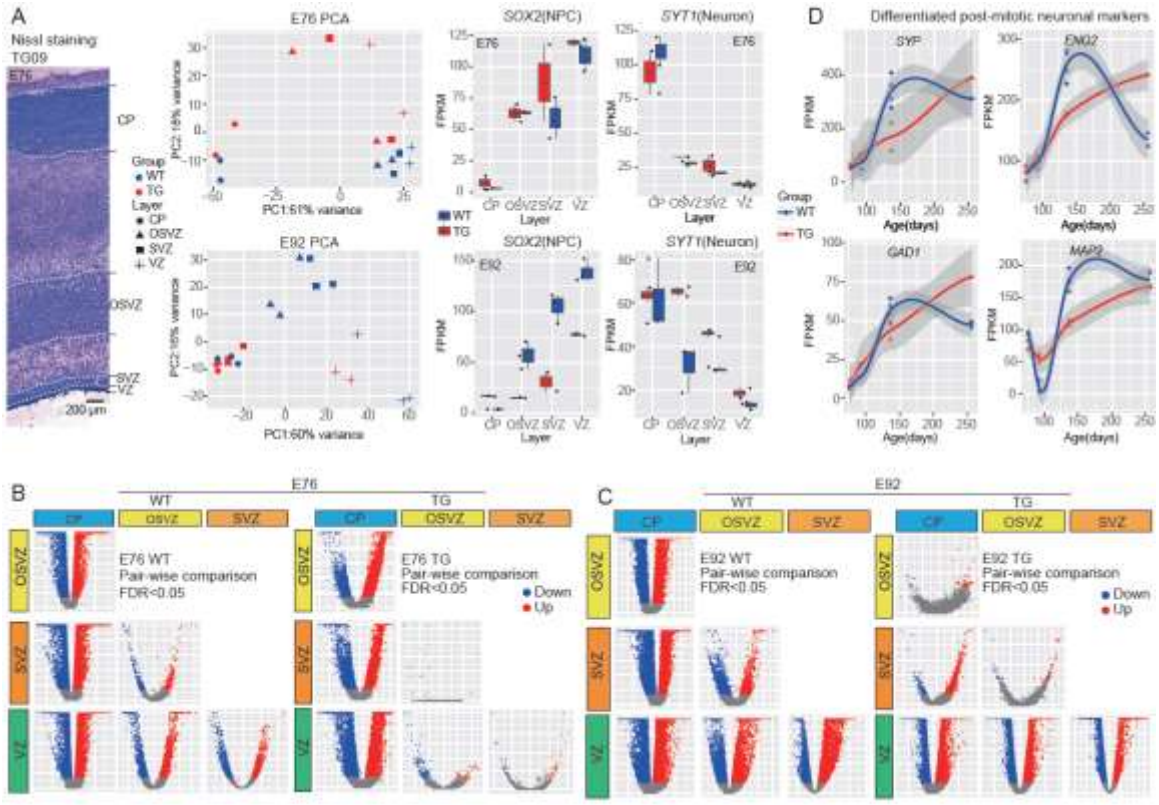

Figure 4. Transcriptome analysis of cortical laminae at E76 and E92. (A) Laser microdissection of cortical laminae and RNAseq analysis. Left panel: Nissl staining of the E76 cortex (TG-09) showing the cortical laminae. Middle panel: the PCA maps of E76 and E92 based on expression levels of all genes; Right panel: cell marker analysis with SOX2 for neuro progenitor cell and SYT1 for neuron. (B) Volcano plots showing pairwise comparisons of gene expression between the indicated laminae of E76. (C) Volcano plots showing pairwise comparisons of gene expression between the indicated laminae of E92. (D) Four mature neuron gene makers showing expression delay in the TG monkeys.

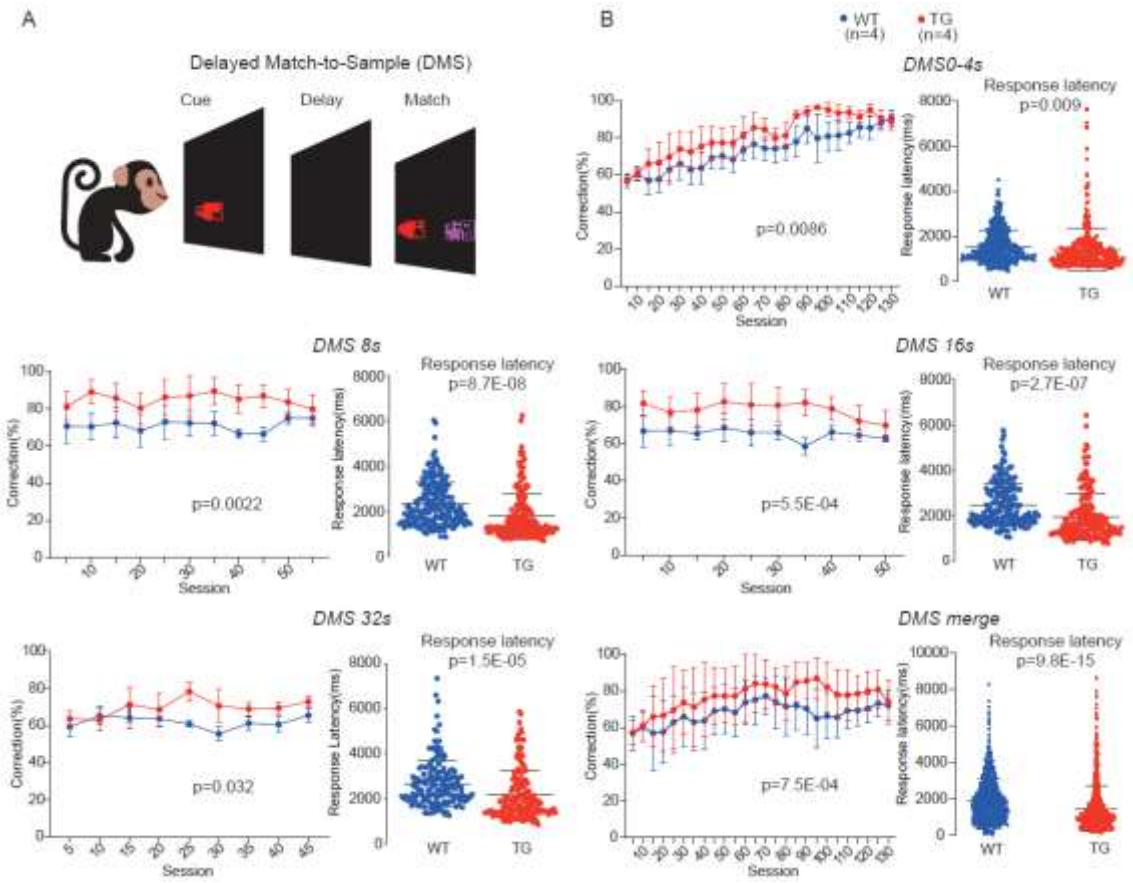

Figure 5. Test of short-term memory using DMS task. (A) Schematic diagram of the DMS task. (B) The results of the DMS trials indicate different performances between the TG and WT monkeys at different delay times including 0-4sec, 8sec, 16sec and 32 sec. The bottom right panel presents the merged DMS data of all delay times. The group effect p values for correction percentage comparison were computed based on the general linear model (GLM), and corrections for multiple tests were conducted using Bonferroni. The p values for reaction time were calculated using two-tailed student t test

Table 1. Information of the generated transgenic monkeys in this study.

Monkey ID	Generation	Sex	Date of Birth	Method of delivery	Status	huMCPH1 copy number
TG_01	F1	Male	2011/6/15	C-section	Live	6
TG_02	F1	Female	2011/6/15	C-section	Live, deceased at 76 days after birth	4
TG_03	F1	Male	/	C-section	Abortion at embryonic 136 days	4
TG_04	F1	Male	/	C-section	Abortion at embryonic 136 days	9
TG_05	F1	Male	2015/6/18	C-section	Live	9
TG_06	F1	Male	2015/6/26	C-section	Live	6
TG_07	F1	Female	2015/6/26	C-section	Live	2
TG_08	F1	Female	2015/6/26	C-section	Live	6
TG_09	F2	Male	/	C-section	Euthanized at embryonic E76 days	5
TG_10	F2	Male	/	C-section	Euthanized at embryonic E92 days	6
TG_11	F2	Male	/	C-section	Euthanized at embryonic E92 days	5